Learning-based Kinematic Calibration using Adjoint Error Model

Nadia Schillreff and Frank Ortmeier
Chair of Software Engineering, Otto-von-Guericke-University Magdeburg, Germany

Keywords: Modeling, Parameter Identification, Product of Exponentials (POE).

Abstract: A learning-based robot kinematic calibration approach based on the product-of-exponentials (POE) formula and Adjoint error model is introduced. To ensure high accuracy this approach combines the geometrical and non-geometrical influences like for e.g. elastic deformations without explicitly defining all physical processes that contribute to them using a polynomial regression method. By using the POE formula for kinematic modeling of the manipulator it is ensured that kinematic parameters vary smoothly and used method is robust and singularity-free. The introduced error parameters are presented in the form of Adjoint transformations on nominal joint twists. The calibration process then becomes finding a set of polynomial functions using regression methods that are able to reflect the actual kinematics of the robot. The proposed method is evaluated on a dataset obtained using a 7-DOF manipulator (KUKA LBR iiwa 7 R800). The experimental results show that this approach significantly reduces positional errors of the robotic manipulator after calibration.

1 INTRODUCTION

For a robot manipulator that is mainly used in repetitive applications (e.g. pick-and-place operations) where the desired poses (position and orientation) of the manipulator's end-effector (EE) can be manually taught, high repeatability is important to successfully perform defined tasks. This ability to repeat a known pose has submilimeter values (e.g. 0.1 *mm* for KUKA LBR iiwa 7 R800) for modern manipulators. However if a task is unique, the robot is mostly given a target pose defined in some relative or absolute coordinate system. Such situations arise often when robot's poses are obtained through a simulation during which the layout of the working environment and a model of the robot are used. This requires special attention to the accuracy of the simulated robot model, and whether it corresponds to the robots actual kinematics.

This process, known as robot calibration, consists of developing a mathematical model and identification of parameters that are able to reflect the actual behavior of the investigated robot and as a result better predict its resulting poses can be build. There are three categories of calibration presented in the literature (Elatta et al., 2004). The first is joint calibration, which is also called first level calibration, where the difference between the actual joints displacements and the encoder signals is considered. Level two involves kinematic calibration, where the robots kinematic parameters are determined. Level three takes into account non-kinematic error sources like elasticity of the links or the backlash of the joints.

One of the most important stages of a calibration procedure is the modeling stage, namely the selection of an apropriate kinematic model and specification of its parameters for error identification. Among the most widely used methods to model robot kinematics is the Denavit-Hartenberg approach (Denavit, 1955) that uses 4 parametrs to describe relations between frames of the manipulator. However, if the robot has consecutive revolute joints with near parallel axes it can lead to convergence problems during parameter identification. Later Hayati and Mirmirani modified this approach by ading an extra parameter of rotation about an axis orthogonal to the plain in which these parallel axes lie(Hayati and Mirmirani, 1985). Other methods that address this problem include for e.g. a Zero-Reference model (Mooring, 1983) and CPC model (Zhuang et al., 1992).

The POE model, which uses twist theory to describe the geometry of each joint and is also a zero reference position method, has been widely used in robotics field. Kinematic parameters of the models based on the POE formula vary smoothly with changes of joint axes, resulting in a continuous parameterization and no singularities for any type of robot. In general methods that use POE models differ by the type of the error assignment: additive (Chen et al., 2014) or multiplicative (Li et al., 2016), and

Schillreff, N. and Ortmeier, F.
Learning-based Kinematic Calibration using Adjoint Error Model.
DOI: 10.5220/0006870403720379
In *Proceedings of the 15th International Conference on Informatics in Control, Automation and Robotics (ICINCO 2018) - Volume 2*, pages 372-379
ISBN: 978-989-758-321-6

by the choice of frames where joint twists are related: global (Okamura and Park, 1996) or local (Chen et al., 2001).

Non-kinematic errors are often attributed to elastic deformations, transmission nonlinearities, and thermal expansion. To account for these errors corresponding effects are analytically expressed with gear or elastic models as in (Klimchik et al., 2015) or (Marie et al., 2013). However, this approach depends on having an accurate representation of the different processes that can potentialy influence the accuracy of the manipulator and inclution of additional parametrs to be identified (e.g. moments of inertia of the robot links, friction parameters). As a result these physical processes are often simplified, leading to inaccuracies in the model.

Instead, learning approaches are proposed to model the behaviour of a robot. This allows us to solve the calibration problem as a function estimation task based on the measured data. The learning approach requires no a-priori knowledge of the physical model. Instead, the model can be obtained directly using measured data. By not attributing errors to specific physical processes we can distribute kinematicic and non-kinematic influences over introduced error parameters. In general errors of the robot's EE may originate from five factors (Liou et al., 1993): environmental (e.g. temperature or the warm-up process), parametric (e.g. Kinematic parameter variation due to manufacturing and assembly errors, influence of dynamic parameters, friction and other nonlinearities), measurement (resolution and nonlinearity of joint position sensors), computational (computer round-off and steady-state control errors) and application (e.g. installation errors). To be able to reflect different influences in the model, experiments that include variations of the relevant factors would have to be conducted. This work considers the influence of only a limited amount of described factors, mainly concentrating on the internal parameters of the robot. However due to the nature of the proposed method, in case the proper experimental data is available the model could be easily extended to include other parameters.

In this paper, a learning based method for robot calibration using Adjoint error model is presented along with a comparison of different modeling approaches. The output of the calibration procedure is a trained model that based on the input variables (e.g. robot joint values and nominal Cartesian position of the EE) would calculate the resulting pose of the manipulator under the influence of kinematic and non-kinematic errors. This model can then be applied to more accurately plan the tasks of the manipulator.

This paper is organised as follows. In Section 2, the forward kinematics based on POE formula along with the Adjoint error model are presented. A method to calculate the values of the introduced error parameters based on measurement data is introduced. We describe different modeling techniques in Section 3. In Section 4, the proposed method is applied to the performance evaluation of a KUKA LBR iiwa 7 R800 manipulator and the modeling thechniques are compared. We conclude our paper in Section 5.

2 ROBOT KINEMATIC AND ERROR MODELING USING POE FORMULA

In this section, a method applied for calculation of error parameters is described. First the POE representation and Adjoint error model is used to describe the robotic manipulator. After that the difference between reference poses of a robots flange measured by a tracking system and the corresponding nominal poses of the robot is used to obtain the values of the introduced error parameters.

2.1 Robot Kinematic Model

According to Brockett (Brockett, 1984), the POE model needs two coordinate frames attached in an arbitrary position. Typicaly a frame S is attached to the robot base link and a tool frame T to the EE. The rigid displacement of T with respect to S can be described by a 4×4 homogeneous matrix $\boldsymbol{g}_{st}$ as:

$$\boldsymbol{g}_{st} = \begin{pmatrix} \boldsymbol{R} & \boldsymbol{p} \\ \boldsymbol{0} & 1 \end{pmatrix} \tag{1}$$

where $\boldsymbol{R}_{3\times3} \in \mathbf{SO}(3)$ is an orthogonal matrix describing coordinate axes of T in S and $\boldsymbol{p}_{3\times1} \in \mathbb{R}_3$ is the position vector of the origin of T in S.

Each joint of the manipulator is associated with a twist $\boldsymbol{\xi}_i, i = 1,\ldots,n$, of the Lie algebra $\mathbf{se}(3)$ of $\mathbf{SE}(3)$ as

$$\widehat{\boldsymbol{\xi}}_i = \begin{pmatrix} \widehat{\boldsymbol{w}}_i & \boldsymbol{v}_i \\ \boldsymbol{0} & 0 \end{pmatrix} \tag{2}$$

where $\boldsymbol{v}_i = [v_{i1}, v_{i2}, v_{i3}]^T \in \mathbb{R}_3$ and $\widehat{\boldsymbol{w}}_i \in \mathbf{so}(3)$ is a skew symmetric matrix of $\boldsymbol{w}_i = [w_{i1}, w_{i2}, w_{i3}]^T \in \mathbb{R}_3$, and is given by:

$$\widehat{\boldsymbol{w}}_i = \begin{pmatrix} 0 & -w_{i3} & w_{i2} \\ w_{i3} & 0 & -w_{i1} \\ -w_{i2} & w_{i1} & 0 \end{pmatrix} \tag{3}$$

The twist $\widehat{\boldsymbol{\xi}}_i$ can also be expresed as a 6×1 vector $\boldsymbol{\xi}_i = (\boldsymbol{v}_i^T, \boldsymbol{w}_i^T)^T \in \mathbb{R}_6$. For a revolute joint, $\boldsymbol{w}_i$ is the direction unit vector of the joint axis and $\boldsymbol{v}_i = \boldsymbol{q}_i \times \boldsymbol{w}_i$, where $\boldsymbol{q}_i$ is an arbitrary point on the joint axis. For a prismatic joint, $\boldsymbol{w}_i = 0$, and $\boldsymbol{v}_i$ gives the unit direction of the joint axis.

Then, the forward kinematic model of a serial robot maping joint variables $\boldsymbol{\Theta} = [\theta_1, \ldots, \theta_n]^T$ to the tool frame displacement $\boldsymbol{g}_{st}$ based on the POE formula can be expressed as (Murray et al., 1994):

$$\boldsymbol{g}_{st} = e^{\widehat{\boldsymbol{\xi}}_1 \theta_1} \ldots e^{\widehat{\boldsymbol{\xi}}_n \theta_n} \boldsymbol{g}_{st_0}, \tag{4}$$

where the matrix exponential $e^{\widehat{\boldsymbol{\xi}}_i \theta_i}$ is the motion generated by joint i with joint variable θ_i , and $\boldsymbol{g}_{st_0}$ denotes the initial tool frame displacement when all joint angles are set to zero.

2.2 Adjoint Error Model

Based on the observed discrepancies between the nominal kinematic model of the robot and measured data, the current robot model has to be extended with error parameters, that can reflect the differences in the pose of the EE.

Li *et al*. proposed a multiplicative Adjoint transformation error of the twist coordinates, referred to as Adjoint error. According to this model the relationship between an actual joint twist and a nominal joint twist, as shown in Figure 1, is given by (Li et al., 2016):

$$\boldsymbol{\xi}^a = \mathrm{Ad}_{eg} \boldsymbol{\xi}^n = \mathrm{Ad}_{e^{\widehat{\boldsymbol{\eta}}}} \boldsymbol{\xi}^n \tag{5}$$

for error parameters $\boldsymbol{\eta} = (\boldsymbol{v}_\eta^T, \boldsymbol{w}_\eta^T)^T \in \mathbf{se}(3)$. Adjoint transformation of the twist $\boldsymbol{\xi}$ with $\boldsymbol{g} = (\boldsymbol{R}, \boldsymbol{p})$ is given by (Murray et al., 1994):

$$\mathrm{Ad}_{\boldsymbol{g}} \boldsymbol{\xi} = \begin{pmatrix} \boldsymbol{R} & \widehat{\boldsymbol{p}}\boldsymbol{R} \\ \mathbf{0} & \boldsymbol{R} \end{pmatrix} \boldsymbol{\xi} \tag{6}$$

And the error of the initial tool frame offset $\boldsymbol{g}_{st_0}$ can be expressed by:

$$\boldsymbol{g}^a_{st_0} = e^{\widehat{\boldsymbol{\eta}}_{st}} \boldsymbol{g}^n_{st_0} \tag{7}$$

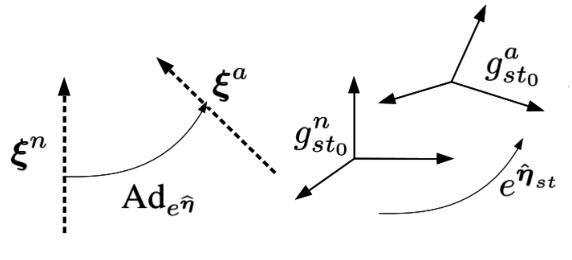

Figure 1: Adjoint error model for joint twists and offset of the tool frame.

2.3 Error Parameters Calculation

After defining an appropriate error model the introduced error parameters should be estimated based on the experimental data. The measured reference pose of a point i, $\boldsymbol{g}^a_{st_i}$, can be written in general form as:

$$\boldsymbol{g}^a_{st_i} = \boldsymbol{f}_H(\boldsymbol{H}), \tag{8}$$

where $\boldsymbol{f}_H$ is a non-linear function of $\boldsymbol{H} = [\boldsymbol{\eta}_1, \ldots, \boldsymbol{\eta}_n, \boldsymbol{\eta}_{st}]$, a vector containing introduced error parameters for each joint and initial tool frame offset. Since these errors are small, this function can be linearized at point $\boldsymbol{H} = \mathbf{0}$. This is equivalent to having all error parameters equal to 0:

$$\boldsymbol{g}^a_{st_i} = \boldsymbol{f}_H(\mathbf{0}) + \mathbf{J}_{\boldsymbol{H}|\mathbf{0}}(\boldsymbol{H} - \mathbf{0}), \tag{9}$$

where $\mathbf{J}_{\boldsymbol{H}|\mathbf{0}}$ is a Jacobian function of $\boldsymbol{f}_H$ with respect to the elements of error vector $\boldsymbol{H}$, evaluated at $\mathbf{0}$ (denoted as $\mathbf{J}_H$ in the following).

Because $\boldsymbol{f}_H(\mathbf{0})$ corresponds to the pose calculated with the nominal parameters $\boldsymbol{g}^n_{st_i}$, given by Equation 4, the difference between nominal and measured pose, $\Delta\boldsymbol{g}_{st_i}$, is:

$$\Delta\boldsymbol{g}_{st_i} = \mathbf{J}_{H_i}\boldsymbol{H} \tag{10}$$

If there are l measurements available, we can present Equation 10 in matrix form as:

$$\Delta\boldsymbol{g}_{st} = \begin{bmatrix} \Delta\boldsymbol{g}_{st_1} \\ \vdots \\ \Delta\boldsymbol{g}_{st_l} \end{bmatrix} = \begin{bmatrix} \mathbf{J}_{H_1} \\ \vdots \\ \mathbf{J}_{H_l} \end{bmatrix} \boldsymbol{H} = \mathbf{J}_H \boldsymbol{H} \tag{11}$$

Under assumption that introduced error parameters are constant, the above equation can be solved with a least squares technique using a left pseudo-inverse matrix of $\mathbf{J}_H$. But considering the need to include the non-geometric influences (which are configuration dependent and as result can not be constant) into developed model, this approach can no longer be used. If, on the other hand, each measurement is considered individually we can find a solution to Equation 10 with a minimum norm using right inverse of $\mathbf{J}_H$:

$$\boldsymbol{H}_i = \mathbf{J}^T_{H_i}(\mathbf{J}_{H_i}\mathbf{J}^T_{H_i})^{-1}\Delta\boldsymbol{g}_{st_i} \tag{12}$$

Solving this equation for every measured-nominal point pair will result in values of the error parameters calculated for every measurement.

It should be notted that the expression for $\Delta\boldsymbol{g}_{st}$ depends on the type of the measurement:

Full Pose Measurements. If the orientation of the EE is measured along with its position, $\Delta\boldsymbol{g}_{st} = [\Delta\boldsymbol{p}, \Delta\boldsymbol{R}]^T$, where positional deviation is $\Delta\boldsymbol{p} = \boldsymbol{p}_a - \boldsymbol{p}_n$, and orientational changes are presented with:

$$\Delta\boldsymbol{R} = log(\boldsymbol{R}_a^{-1}\boldsymbol{R}_n)^\vee \tag{13}$$

$$log(\boldsymbol{R}) = \frac{\theta(\boldsymbol{R})}{2sin(\theta(\boldsymbol{R}))}(\boldsymbol{R} - \boldsymbol{R}^T) \quad (14)$$

where

$$\theta(\boldsymbol{R}) = arccos\left(\frac{trace(\boldsymbol{R}) - 1}{2}\right) \quad (15)$$

Position Only Measurements. In this case, not only $\Delta \boldsymbol{g}_{st}$ consists of positional deviation only, but also we cannot identify rotational errors in the initial tool frame orientation from position measurements only.

3 MODELING OF THE ERROR PARAMETERS

After calculating the values of the error parameters for every point pair, we can construct such a model that would reflect the behavior of the real robot as precisely as possible and at the same time remain general enough to be able to be applied to the new data. For this purpose the defined error parameters are modeled and trained using a fraction of the experimental data.

3.1 Data Preprocessing

For every introduced error parameter regression analysis is used to predict its value depending on input variables. These variables also called independent variables are denoted by $\boldsymbol{X}$. In order to model nonlinear relationships, input variables can be extended by $\boldsymbol{X} = [x_1, x_1^2 \dots x_1^p \dots x_n^p]$, where p is the degree of polynomial.

If a feature has a variance that is orders of magnitude larger than others, it might dominate the objective function and skew the estimator preventing it from learning from other features correctly. It also influences the convergence of steepest descent algorithms, which do not possess the property of scale invariance.

To prevent such behaviour, centering and scaling should be applied independently to each input variable by computing the relevant statistics on the samples in the training set:

$$x_i' = \frac{x_i - \bar{x_i}}{\sigma}, \quad (16)$$

where $\bar{x_i} = \frac{1}{s}\sum x_i$ is the mean value of a dataset of size s. Mean and standard deviation of the training set are then used to transform the values of the training set.

3.2 Regression Analysis

One of the basic forms of regression analysis is linear regression. It uses a Least Square Method to find a model that fits the observed data by minimizing the sum of the squared deviations between the observation and an estimator (Rawlings et al., 2001):

$$min||\boldsymbol{X}\boldsymbol{\omega} - y||_2^2, \quad (17)$$

where y represents the target variable, and ω regression coefficients.

By introducing a higher degree polynomial we can potentially better fit the fluctuations in the observed data. On the other hand it can lead to over-fitting and as a result poor performance on new data. Therefore additional measures should be made to ensure better performance.

3.2.1 Ridge Regression

Ridge regression (Hoerl and Kennard, 1970) is a technique that uses regularization by minimizing a penalized residual sum of squares (Equation 18). This approach is effective in case of highly correlated input variables.

$$min||\boldsymbol{X}\boldsymbol{\omega} - y||_2^2 + \lambda_R||\boldsymbol{\omega}||_2^2, \quad (18)$$

where $\lambda_R \geq 0$ is the shrinkage parameter that controls the amount of regularization. Larger values of λ_R would relult in lower regression coefficients, and minimize the impact of irrelevant input variables on the trained model to avoid overfitting in case of collinearity.

3.2.2 LASSO

LASSO (Least Absolute Shrinkage and Selection Operator) is a regularization and variable selection method that adds a factor of sum of absolute value of coefficients in the optimization objective (Tibshirani, 1996):

$$\frac{||\boldsymbol{X}\boldsymbol{\omega} - y||_2^2}{s} + \lambda_L||\boldsymbol{\omega}||_1, \quad (19)$$

where a tuning parameter, $\lambda_L \geq 0$, controls the strength of the penalty. When $\lambda_L = 0$ no parameters are eliminated and the estimate is equivalent to linear regression. With the increase of this parameter, more input variables have coefficient equal to zero and are excluded from the model.

Lasso's characteristic to push its weights to zero is its advantage over Ridge regression, because it can perform regression and variable selection at the same time.

3.2.3 Elastic Net

If there are input variables that are higly correlated between each other, LASSO selects one variable from each group and ignores the others. Elastic Net (Zou and Hastie, 2005) is an extension of LASSO that overcomes its limitations with a combination of LASSO and Ridge regression methods. This method minimizes the following objective function:

$$\frac{||\boldsymbol{X}\boldsymbol{\omega}-y||_2^2}{s}+\lambda_{E2}||\boldsymbol{\omega}||_2^2+\lambda_{E1}||\boldsymbol{\omega}||_1, \tag{20}$$

where $\lambda_{E1} \geq 0$ and $\lambda_{E2} \geq 0$ are two regularization parameters. By adding a quadratic part to the penalty, Elastic Net stabilizes the selection from correlated variables. This allows not only to have regularization properties of Ridge, but also result in a sparse model with few non-zero weights like LASSO regression.

3.3 Model Training

To evaluate the performance of the models the available data set is split into training and testing sets: the training set is used to determine the regression coefficients of the models and for tuning model parameters λ, and the performance evaluation is done on the test set that was not used during modeling.

To determine the regularization parameters k-fold cross-validation (CV), during which the training set is split into k smaller sets, is used. Then for each of these k sets a model is trained using $k-1$ of the remaining sets, and the resulting model is validated on the remaining part of the set. The resulting performance measure of the k-fold CV is calculated as the average of the values computed in the loop. Because there are two tuning parameters in the Elastic Net (λ_{E1} and λ_{E2}), the CV is done on a two-dimensional surface. Those parameters that result in the smallest CV error are chosen for model training.

To evaluate the performance of regression models, R^2 metric (the coefficient of determination) is used. It provides a measure of how well test data are likely to be predicted by the model. If $\hat{y}_i$ is the predicted value, then:

$$R^2(y,\hat{y}) = 1-\frac{\sum(y_i-\hat{y}_i)^2}{\sum(y_i-\bar{y})^2} \tag{21}$$

According to the presented calibration approach the identification of error parameters for every point in the training dataset and subsequent learning of the regression models is required. The needed computational time is therefore bigger compared to the conventional calibration methods, but considering that it is conducted off-line, the computational time is not so critical.

4 EXPERIMENT EVALUATION

In order to verify accuracy and effectiveness of the presented error modeling approach, the proposed method is evaluated on an example of a 7-DOF KUKA LBR iiwa 7 R800 robot. The used data set was provided by Siemens Healthcare GmbH.

4.1 Experimental Setup

We calibrate a KUKA LBR iiwa 7 R800 robot using a FARO laser tracking system to measure the position of a SMR target, rigidly mounted on the robot flange. The accuracy of the laser tracker is up to 0.015 *mm*. The measured dataset includes position data from 875 points in 170 × 520 × 520 *mm* measuring volume. The data from the tracker was transformed into the coordinate system of the robot using a least mean square and Singular Value Decomposition approach (Lorusso et al., 1995). The nominal joint twists of KUKA LBR iiwa 7 R800 used to get nominal values of the EE are listed in Table 1.

Table 1: KUKA LBR iiwa 7 R800 nominal parameters (mm).

ξ_1^n	(0, 0, 0, 0, 0, 1)
ξ_2^n	(-340, 0, 0, 0, 1, 0)
ξ_3^n	(0, 0, 0, 0, 0, 1)
ξ_4^n	(740, 0, 0, 0, -1, 0)
ξ_5^n	(0, 0, 0, 0, 0, 1)
ξ_6^n	(-1140, 0, 0, 0, 1, 0)
ξ_7^n	(0, 0, 0, 0, 0, 1)
$\boldsymbol{g}_{st_0}^n$	$\begin{pmatrix}1 & 0 & 0 & 0\\ 0 & 1 & 0 & 0\\ 0 & 0 & 1 & 1266\\ 0 & 0 & 0 & 1\end{pmatrix}$

4.2 Model Comparisson

For the process of model building the given dataset was split into training (60 points) and testing (815 points) sets. Using Equation 12 we find values of the introduced error parameters for every data point in training set. As input parameters for the regression models take the nominal Cartesian position of the EE (X,Y,Z) and the robot joint angles $(\theta_1,\ldots,\theta_7)$. These parameters are considered as basic inputs that do not depend on the particular robot structure and can be easily obtained without access to the robot controller. In order to choose the hyperparameters for the regression models 5-fold CV was performed on the training set. In the final step of the calibration, after error parameter models are trained, the resulting estimators can then be used to estimate the values of the identified error parameters for the testing set.

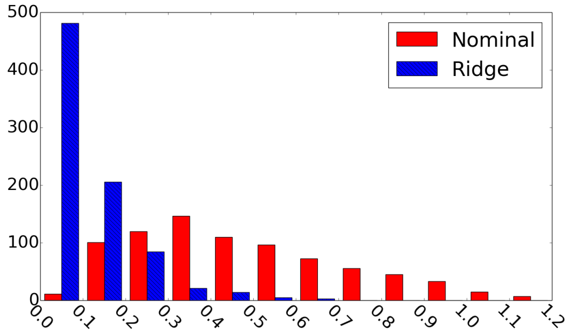

Figure 2: Frequency histogram of the distance error (mm) for Ridge regression.

To illustrate the results of the modeling, error parameters were estimated by the trained models for the test set and the corrected positions of the EE were calculated. The frequency plot of the resulting positional errors, measured as the distance between the nominal and measured position alongside with the distance from modeled to measured position, for Ridge (Figure 2), LASSO (Figure 3), and Elastic Net regression (Figure 4) shows significant shift of error distribution towards zero.

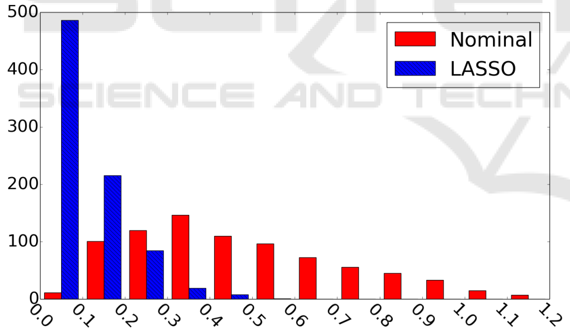

Figure 3: Frequency histogram of the distance error (mm) for LASSO regression.

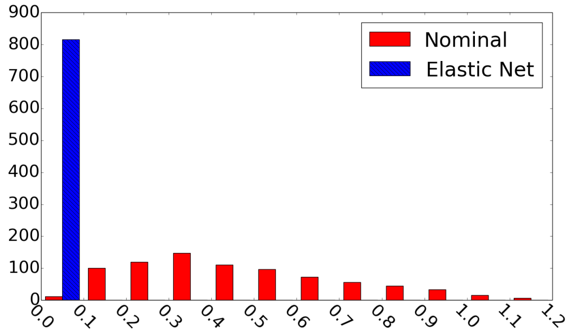

Figure 4: Frequency histogram of the distance error (mm) for Elastic Net regression.

Table 2: Distance error (mm) before and after modeling.

Error	Measured	Modeled		
		Ridge	LASSO	Elastic Net
mean	0.48	0.11	0.11	0.03
std	0.25	0.10	0.09	0.01
max	1.17	0.68	0.54	0.06

To better compare the results of the error modeling, Table 2 combines the statistical information for the modeled error parameters. A substantial decrease in standard deviation values for all models in comparison to the nominal robot values can be observed. It can also be seen that Elastic Net regression showed best results in comparisson to other models.

4.3 Size of the Training Set

To investigate how the size of the training set influences the performance of the modeling approaches, error models were trained using $[25, 35, \ldots, 95]$ points from the available dataset. To ensure that each point was used for training and testing at least once 5-fold CV was used. To account for the variance in the algorithm itself the CV procedure was run 25 times, giving an estimate of the performance of the algorithm on the dataset and an estimation of how robust its performance is.

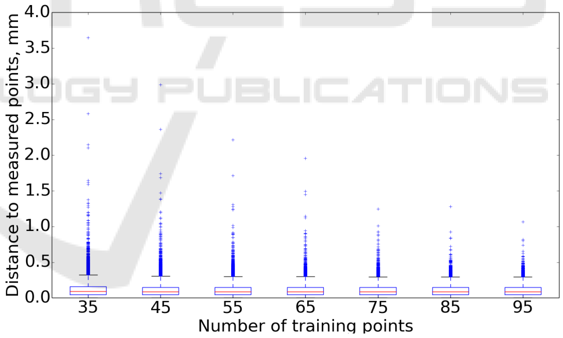

Figure 5: Distance error for the test set for different number of training points for Ridge regression.

The box plots of the resulting positional errors for Ridge (Figure 5), LASSO (Figure 6), and Elastic Net regression (Figure 7) show that the mean value stays almost the same and only the maximum values change. From the Table 3, that presents the statistical information of the regression models comparisson, we can see that Elastic Net shows the best results.

5 CONCLUSIONS

A learning based approach using the Adjoint error model and POE formula was presented and evalu-

Table 3: Distance error (mm) comparisson for different sizes of training sets based on 25 repetitions.

Size of the training set	Ridge			LASSO			Elastic Net		
	mean	std	max	mean	std	max	mean	std	max
35	0.12	0.12	3.65	0.10	0.09	2.87	0.03	0.03	0.72
45	0.11	0.10	2.99	0.10	0.08	1.39	0.02	0.02	0.37
55	0.11	0.09	2.22	0.10	0.08	0.99	0.02	0.01	0.33
65	0.11	0.07	1.95	0.10	0.08	0.89	0.02	0.01	0.06
75	0.11	0.08	1.25	0.10	0.08	0.85	0.01	0.01	0.06
85	0.11	0.08	1.28	0.10	0.07	0.64	0.01	0.01	0.05
95	0.10	0.08	1.07	0.10	0.07	0.61	0.01	0.01	0.05

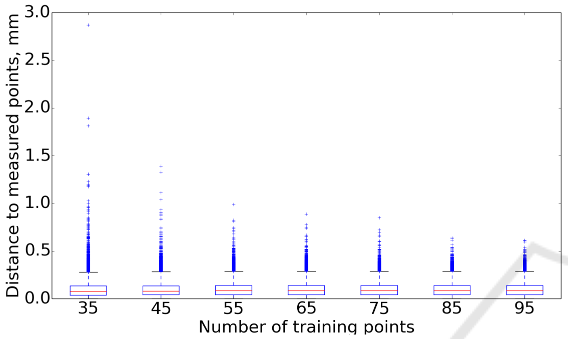

Figure 6: Distance error for the test set for different number of training points for LASSO regression.

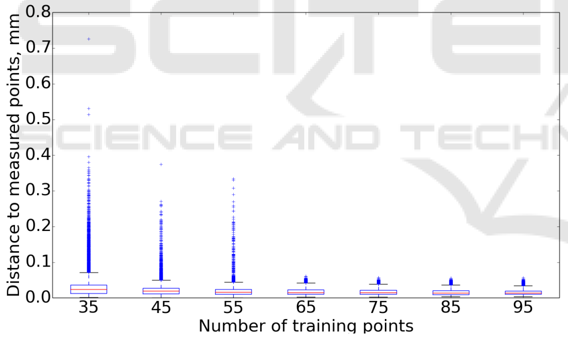

Figure 7: Distance error for the test set for different number of training points for Elastic Net regression.

ated on example of KUKA LBR iiwa 7 R800. Kinematic and non-kinematic influences were included in the calibration model without explicitly using physical models, by distributing their influence over introduced error parameters. Regression analysis was then used to predict their values for new data. Three regression methods were compared on the number of training points and resulting distance error using a dataset containing positional measurements of the robot flange. As a result of this evaluation, all three models showed decrease in distance errors at the EE having low mean values over different number of training points. The Elastic Net model showed best results by significantly improving the absolute accuracy of the manipulators tool position using a model depending on nominal Cartesian position of the EE and joint configurations of the robot. An example model trained with 60 points reduced the mean value of the positional errors from 0.4808 *mm* to 0.0337 *mm* and the maximum value from 1.1513 *mm* to 0.0601 *mm*.

As any learning based approach the proposed method highly depends on the training data. As part of the future work influences of different input parameters will be evaluated by designing different experiments. Another important goal is to find some optimal distribution and minimal number of points necessary for training to reach needed accuracy. The dynamic robot calibration, in which the impact of the motion is considered, can also be applied using the proposed method, if apropriate input parameters are used for building the error model.

REFERENCES

Brockett, R. W. (1984). Robotic manipulators and the product of exponentials formula. In *Mathematical theory of networks and systems*, pages 120–129. Springer.

Chen, G., Wang, H., and Lin, Z. (2014). Determination of the identifiable parameters in robot calibration based on the poe formula. *IEEE Transactions on Robotics*, 30(5):1066–1077.

Chen, I.-M., Yang, G., Tan, C. T., and Yeo, S. H. (2001). Local poe model for robot kinematic calibration. *Mechanism and Machine Theory*, 36(11-12):1215–1239.

Denavit, J. (1955). A kinematic notation for low pair mechanisms based on matrices. *ASME J. Appl. Mech.*, 22:215–221.

Elatta, A., Gen, L. P., Zhi, F. L., Daoyuan, Y., and Fei, L. (2004). An overview of robot calibration. *Information Technology Journal*, 3(1):74–78.

Hayati, S. and Mirmirani, M. (1985). Improving the absolute positioning accuracy of robot manipulators. *Journal of Robotic Systems*, 2(4):397–413.

Hoerl, A. E. and Kennard, R. W. (1970). Ridge regression: Biased estimation for nonorthogonal problems. *Technometrics*, 12(1):55–67.

Klimchik, A., Furet, B., Caro, S., and Pashkevich, A. (2015). Identification of the manipulator stiffness model parameters in industrial environment. *Mechanism and Machine Theory*, 90:1–22.

Li, C., Wu, Y., Löwe, H., and Li, Z. (2016). Poe-based robot kinematic calibration using axis configuration space and the adjoint error model. *IEEE Transactions on Robotics*, 32(5):1264–1279.

Liou, Y. A., Lin, P. P., Lindeke, R. R., and Chiang, H.-D. (1993). Tolerance specification of robot kinematic parameters using an experimental design techniquethe taguchi method. *Robotics and computer-integrated manufacturing*, 10(3):199–207.

Lorusso, A., Eggert, D. W., and Fisher, R. B. (1995). A comparison of four algorithms for estimating 3-d rigid transformations. In *Proceedings of the British Conference on Machine Vision*, pages 237–246.

Marie, S., Courteille, E., and Maurine, P. (2013). Elasto-geometrical modeling and calibration of robot manipulators: Application to machining and forming applications. *Mechanism and Machine Theory*, 69:13–43.

Mooring, B. (1983). The effect of joint axis misalignment on robot positioning accuracy. In *Proceedings of the ASME International Computers in Engineering Conference and Exhibition*, pages 151–155.

Murray, R. M., Li, Z., Sastry, S. S., and Sastry, S. S. (1994). *A mathematical introduction to robotic manipulation*. CRC press.

Okamura, K. and Park, F. C. (1996). Kinematic calibration using the product of exponentials formula. *Robotica*, 14(04):415–421.

Rawlings, J. O., Pantula, S. G., and Dickey, D. A. (2001). *Applied regression analysis: a research tool*. Springer Science & Business Media.

Tibshirani, R. (1996). Regression shrinkage and selection via the lasso. *Journal of the Royal Statistical Society. Series B (Methodological)*, pages 267–288.

Zhuang, H., Roth, Z. S., and Hamano, F. (1992). A complete and parametrically continuous kinematic model for robot manipulators. *IEEE Transactions on Robotics and Automation*, 8(4):451–463.

Zou, H. and Hastie, T. (2005). Regularization and variable selection via the elastic net. *Journal of the Royal Statistical Society: Series B (Statistical Methodology)*, 67(2):301–320.